

There have been a number of reports on the nucleotide sequence analysis of the rearranged NCCRs to differentiate patient-dependent JCV variants for PML diagnosis and/or to examine the molecular pathogenesis of JCV [14, 19–29]. However, since multiple variants are frequently released into the CSF of many PML patients, NCCR typing requires molecular cloning of viral DNA, nucleotide sequencing, and *in silico* analysis of mutations [14, 19–24]. Thus, the analysis of NCCR patterns is labor-intensive, time-consuming, and highly expensive, making it difficult to be undertaken routinely.

High-resolution melting (HRM) analysis is a rapid, sensitive, closed-tube technique for the detection of DNA sequence variations. It relies on fluorescence melting curves obtained from the transition of double-stranded DNA to single-stranded DNA as a result of temperature increases [30]. HRM is used as a high-throughput and low-cost method for mutation scanning and genotyping in clinical practice and risk assessment, including the characterization of viral genomes [31]. This study was undertaken to develop and evaluate an HRM-based analysis technique to distinguish the NCCR patterns of JCV variants.

## Materials and methods

### CSF specimens

The study protocol was approved by the Ethical Committee for Biomedical Science in the National Institute of Infectious Diseases (approval number 388 and 389). CSF specimens were collected by lumbar puncture from 163 patients after informed consent from the patients or their family members was obtained, and then transferred from the respective hospitals to the Department of Virology 1, National Institute of Infectious Diseases, Tokyo, Japan, for the clinical testing of JCV DNA as a part of routine medical practice. Twelve of the subjects were diagnosed with PML on the basis of neurological symptoms, magnetic resonance imaging patterns, and the detection of JCV DNA in the initial CSF testing. One hundred fifty-one patients were negative for CSF JCV as judged by real-time PCR testing.

### DNA extraction and real-time PCR

Total DNA was extracted from CSF specimens using a QIAamp DNA Blood Mini Kit (QIAGEN, Valencia, CA), and the JCV DNA copy number in each sample was determined using a real-time PCR assay as described previously [24, 32].

### Cloning and sequencing of NCCRs

The NCCRs were amplified by nested PCR using CSF DNAs from 12 PML patients and were cloned into a plasmid

vector as reported earlier [24]. Sequencing of 96 NCCR clones (8 clones/patient) from both sides of the insert was performed using universal primers, and the nucleotide sequences were compared to that of the archetype CY strain recovered from a healthy Japanese individual (GenBank: AB038249.1) [33] using the CLC Genomics Workbench 6.0.1 software program (CLC bio, Aarhus, Denmark) as described previously [24]. In each specimen, at least 5 of the 8 NCCR clones had identical sequences and were used as representative clones for HRM typing.

### HRM analysis of cloned NCCRs

The viral genome of archetype JCV (CY strain) was provided by the RIKEN BRC through the National Bio-Resource Project of MEXT, Japan. A pair of primers, JCHRM-F (5'-CCT CCT AAA AAG CCT CCA CG-3') and JCHRM-R (5'-AGA AGC CTT ACG TGA CAG C-3'), which correspond to nucleotides 5064–5083 and 282–300 within the circular genome of JCV CY strain, respectively, was designed to anneal to highly conserved sequences adjacent to the NCCR. Custom-synthesized and cartridge-purified primers were obtained from Life Technologies (Gaithersburg, MD). Real-time PCR amplification and HRM analysis were carried out in a single tube and a single run using a LightCycler Nano System and ResoLight, a DNA-intercalating fluorescent dye (Roche, Penzberg, Germany) according to the protocols supplied by the manufacturers. For HRM analysis of the plasmid-cloned NCCRs, the reaction was performed in a total volume of 20  $\mu$ L containing 10  $\mu$ L of the LightCycler 480 High Resolution Melting Master (Roche, Penzberg, Germany), 0.8  $\mu$ L each of the 10  $\mu$ M forward and reverse primers, 2  $\mu$ L of 25 mM magnesium chloride (Roche), and 2  $\mu$ L of the plasmid DNA (10 ng/reaction). Amplification and real-time fluorescence detection were performed using a LightCycler Nano Instrument (Roche), and the cycling conditions were 95  $^{\circ}$ C for 10 min, followed by 30 cycles of 95  $^{\circ}$ C for 10 s, 60  $^{\circ}$ C for 25 s, and 72  $^{\circ}$ C for 15 s. The optimal cycle conditions and magnesium chloride concentration were determined by pilot experiments to prevent background noise due to nonspecific amplification. HRM analysis was performed immediately after cycling by first heating to 95  $^{\circ}$ C, cooling to 40  $^{\circ}$ C, heating again to 65  $^{\circ}$ C (all at 4  $^{\circ}$ C/s), and then melting at 0.05  $^{\circ}$ C/s with continuous acquisition of fluorescence until 95  $^{\circ}$ C. The HRM data were analyzed using the LightCycler Nano Software (Roche) following the manufacturer's instructions. The melting curves were normalized and temperature shifted to allow samples to be directly compared. Difference plots were generated by selecting the reference DNA, converting the melting profile to a baseline, and normalizing the melting profiles of the other samples against this sample.

The specificities of the amplified products were confirmed by the conventional direct sequencing method.

#### HRM analysis of JCV DNA in CSF samples

For mutation scanning of small amounts of viral DNA in clinical specimens, the NCCRs were pre-amplified by conventional PCR using CSF DNAs from 12 PML patients and 151 CSF JCV-negative patients. To prevent over-amplification, the JCV-positive CSF DNAs were diluted to less than  $10^3$  copies per reaction and were used as PCR templates. The JCV-negative CSF DNAs were directly subjected to PCR without dilution. The outer primers, A1 (5'-TCC ATG GAT TCC TCC CTA TTC AGC ACT TTG T-3') and A2 (TTA CTT ACC TAT GTA GCT TT-3'), have been described previously [28]. PCR was performed using a high-fidelity DNA polymerase with proofreading activity in a 50- $\mu$ L reaction mixture as reported previously [24, 34]. Amplification was performed in a thermal cycler (PCR Thermal Cycler Dice; Takara, Shiga, Japan) with initial denaturation at 98 °C for 1 min, followed by 40 cycles of 98 °C for 10 s, 55 °C for 30 s, and 72 °C for

30 s, and a final extension at 72 °C for 5 min. The PCR product was diluted tenfold with PCR-grade water and subjected to the real-time PCR-HRM assay as described above.

#### Nucleotide sequence accession numbers

NCCR sequences were submitted to the DNA Data Bank of Japan (DDBJ) and were assigned the accession numbers GenBank/EMBL/DDBJ: AB841277–AB841306.

## Results

#### Nucleotide sequence analysis of the NCCRs of JCV variants in CSF specimens from PML patients

The first series of analyses was conducted to examine the NCCR patterns of JCV DNA detected in CSF specimens from PML patients, using a conventional cloning and sequencing approach (Table 1). The viral loads in CSF specimens of 12 PML patients ranged between  $2.06 \times 10^3$

**Table 1** PML patients and representative NCCR patterns of JCV variants detected in CSF specimens

Patient no.	Underlying disease	CSF viral load (copies/mL)	NCCR clone	Nucleotide sequence composition <sup>a</sup>		
				Deletion <sup>b</sup>	Insertion	Single-base difference <sup>c</sup>
1	HIV infection	$2.06 \times 10^3$	Os-1-1	60-78	81-108, 49-57	NA
2	HIV infection	$2.26 \times 10^3$	Tk-5-2	108-123, 128-175	NA	NA
3	HCV-related liver disease	$3.06 \times 10^3$	Tk-16-4	91-159	158-194, 59-66, 60-92, 252-258	T91C, C159A, G226A
4	HIV infection	$2.58 \times 10^4$	Ng-21-2	203-252	NA	NA
5	HIV infection	$4.27 \times 10^4$	Tk-24-1	116-178	181-205, 46-75, 98-113, 179-206, 47-113	NA
6	HIV infection	$2.69 \times 10^5$	Ir-30-1	54-76	NA	C85G
7	Primary immunodeficiency syndrome	$5.21 \times 10^5$	St-29-4	37-38, 41-60, 141-169, 220-257	77-142	NA
8	HIV infection	$5.36 \times 10^5$	Hs-32-2	124-130	133-141, 40-107, 108-121, 30-34	T107A, G112T, G141A, C159A, G217A
9	NA	$9.93 \times 10^5$	Fo-39-1	112-167, 200-201	103-114, 168-199, 202-219, 30-111, 103-114	NA
10	HIV infection	$1.49 \times 10^8$	Ac-46-1	76-168, 189-224	37-86, 169-185, 163-166, 68-86	NA
11	HIV infection	$3.15 \times 10^8$	St-58-2	94-182	183-209, 49-91, 181-191, 49-91, 181-207	A208T, G217A
12	Acute lymphoblastic leukemia	$4.85 \times 10^8$	Os-47-1	88-178, 213-220	179-198, 108-150, 71-76	NA

PML, progressive multifocal leukoencephalopathy; NCCR, non-coding control region; JCV, JC virus; CSF, cerebrospinal fluid; HCV, hepatitis C virus; NA, not applicable

<sup>a</sup> The nucleotide numbers corresponding to the nucleotide positions within the JCV genome of the archetype CY strain are shown

<sup>b</sup> "60-78" indicates that 5' and 3' nucleotide positions 60-78 are deleted

<sup>c</sup> "T91C" indicates that T at the nucleotide position 91 in the archetype NCCR is C

**Table 2** Frequency and sequence differences in the rearranged NCCRs cloned from CSF specimens of PML patients

Patient no.	NCCR clone	Accession no.	Frequency	Size (bp)	Nucleotide sequence composition <sup>a</sup>		
					Deletion	Insertion <sup>b</sup>	Single-base difference <sup>c</sup>
1	Os-1-1	AB841277	6/8	285	-	-	-
	Os-1-7	AB841278	1/8	285	NA	NA	T222C
	Os-1-3	AB841279	1/8	285	NA	NA	A151G, G163A
2	Tk-5-2	AB841280	7/8	203	-	-	-
	Tk-5-1	AB841281	1/8	203	NA	NA	C56A
3	Tk-16-4	AB841282	6/8	283	-	-	-
	Tk-16-2	AB841283	1/8	283	NA	NA	A211G
	Tk-16-10	AB841284	1/8	283	NA	NA	A92G
4	Ng-21-2	AB841285	7/8	217	-	-	-
	Ng-21-5	AB841286	1/8	217	NA	NA	A56G
5	Tk-24-1	AB841287	7/8	370	-	-	-
	Tk-24-8	AB841288	1/8	370	NA	NA	A293G
6	Ir-30-1	AB841289	8/8	244	-	-	-
7	St-29-4	AB841290	5/8	244	-	-	-
	St-29-7	AB841291	2/8	264	NA	43-60	NA
	St-29-2	AB841292	1/8	264	NA	43-60	T91C
8	Hs-32-2	AB841293	6/8	356	-	-	-
	Hs-32-8	AB841294	1/8	356	NA	NA	C90G, T205G
	Hs-32-10	AB841295	1/8	355	NA	NA	del29, T205G
9	Fo-39-1	AB841296	6/8	365	-	-	-
	Fo-39-5	AB841297	1/8	365	NA	NA	A152G
	Fo-39-7	AB841298	1/8	365	NA	NA	T353C
10	Ac-46-1	AB841299	5/8	228	-	-	-
	Ac-46-8	AB841300	1/8	228	NA	NA	C116T
	Ac-46-2	AB841301	1/8	230	NA	232-233	NA
	Ac-46-5	AB841302	1/8	189	62-100	NA	NA
11	St-58-2	AB841303	6/8	329	-	-	-
	St-58-3	AB841304	2/8	242	122-140, 151-167, 172-177, 240-284	NA	C149G, A150G, A179G
12	Os-47-1	AB841305	7/8	237	-	-	-
	Os-47-9	AB841306	1/8	248	NA	88-90, 159-163, 156-158	NA

NCCR, non-coding control region; CSF, cerebrospinal fluid; PML, progressive multifocal leukoencephalopathy; NA, not applicable

<sup>a</sup> The NCCR sequences were compared to those of the frequent patterns in each CSF specimen (minus symbols)

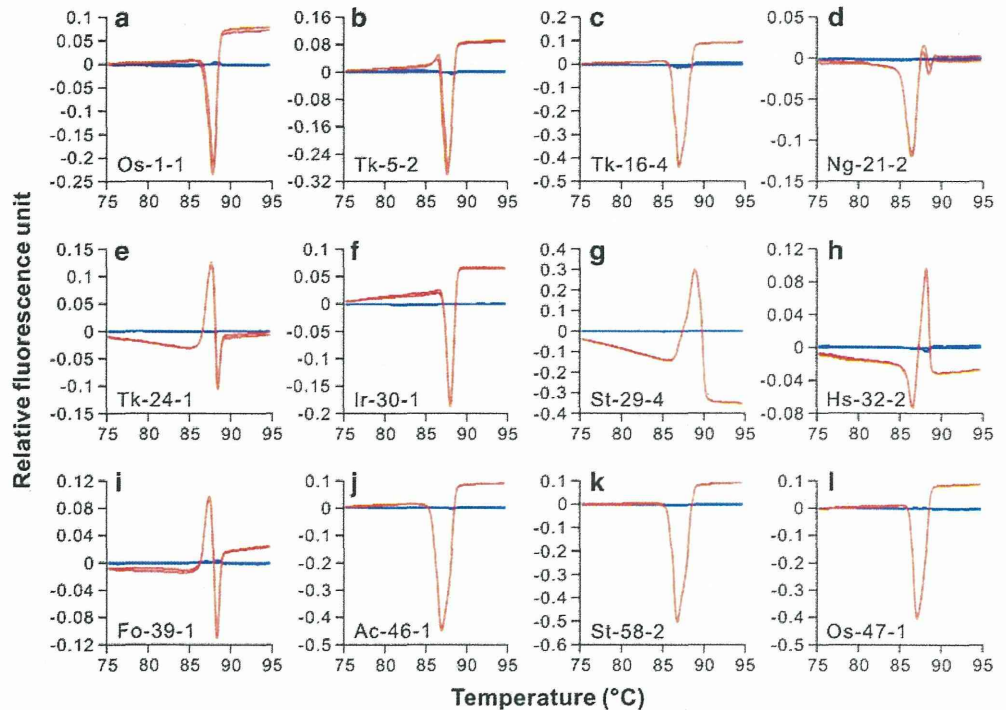
<sup>b</sup> The nucleotide numbers corresponding to the nucleotide positions within the JCV genome of the archetype CY strain are shown as the sequences were partially deleted in some frequent patterns

<sup>c</sup> "T222C" indicates that T at the nucleotide position 222 in the frequent NCCR pattern is C

and  $4.85 \times 10^8$  copies/mL. The DNA fragments containing the NCCR were amplified by nested PCR, and their nucleotide sequences were analyzed after plasmid cloning. The NCCR patterns of the representative clones in each specimen are shown. When compared to the archetype sequence, all patterns had deletions, mainly in the C (nucleotides 60-114) and/or D (nucleotides 115-180) regions within the NCCR. Partial deletions were also observed in other regions within the NCCRs of 7 of the 12

clones. In 9 of the 12 NCCRs, short fragments were inserted into the deleted regions, resulting in duplications. Single-nucleotide differences within the NCCR were also identified in 4 of the 12 NCCRs. Table 2 shows a comparison of the nucleotide sequences between the representative and low-frequency NCCR patterns. In all PML patients, except patient 6, multiple NCCR patterns were identified in the same CSF specimen. The sequence compositions of these NCCRs differed among patients. These

**Fig. 1** Comparisons of HRM profiles between the archetype and rearranged NCCRs. The real-time PCR-HRM assay was performed on the archetype NCCR (blue lines) and the rearranged NCCRs listed in Table 1 (red lines) in duplicate. Differences in fluorescence were determined by comparison with the data of the archetype NCCR. Similar results were obtained from two other experiments (color figure online)



data suggest that the NCCRs of JCV from each individual exhibited patient-dependent mutational patterns.

Detection of NCCR mutations by real-time PCR-HRM analysis

The next series of analyses was carried out to examine whether the real-time PCR-HRM assay could detect the mutations in the sequence-determined NCCRs. The archetype and representative NCCRs in Table 1 were amplified by real-time PCR, and the temperature-shifted difference plots of each product were determined by HRM analysis. Baseline data were obtained from the archetype NCCR (Fig. 1, blue lines). When the rearranged NCCRs were used as PCR templates, HRM profiles clearly deviated from the baseline in the positive and/or negative direction on the y-axis during the temperature shifts (Fig. 1, red lines). Figure 2a shows the results of the HRM profiles for each NCCR with reference to the rearranged NCCR sequence. When the data from the NCCR clone Os-1-1 were set as a baseline, the HRM profiles of these sequences appeared to differ from those of the other clones (Fig. 2a). In addition, the HRM profiles of the NCCRs differed from each other when any NCCR clones were set as the baseline (data not shown). The experiments shown in Fig. 2b were performed to determine whether the real-time PCR-HRM assay could discriminate between the minor sequence differences in NCCR clones derived from the same CSF specimen. The real-time PCR-HRM analyses

were performed using the representative and other DNA clones as PCR templates (Table 2). The HRM profiles of the minor NCCRs were compared with reference to those of the representative clones as a baseline. Although the HRM profiles seemed to be similar, the NCCR patterns could be discriminated in all template combinations except NCCR clones Tk-16-10 and Tk16-4 (94.4 %). These data demonstrate that the real-time PCR-HRM can be used for the differentiation of DNA sequences of the archetype and rearranged NCCRs.

Scanning of NCCR mutations within the JCV genome detected in CSF specimens from PML patients by real-time PCR-HRM analysis

To analyze low-copy JCV DNA in clinical specimens, the real-time PCR-HRM assay was improved by the use of a nested PCR technique (hereafter “nested PCR-HRM”). When the pre-amplified products of conventional PCR using outer primers were used as templates, nested PCR-HRM was capable of detecting and scanning at least 20 copies of NCCR fragment per reaction. The nested PCR-HRM analysis was performed on JCV-positive and -negative CSF DNAs (12 and 151 specimens, respectively). Baseline data were obtained from the archetype NCCR (Fig. 3, blue lines). The assay detected JCV NCCR in all JCV-positive specimens, and HRM patterns of JCV NCCRs from these samples (Fig. 3, red lines) appeared to differ from those of the archetype JCV (Fig. 3, blue lines).

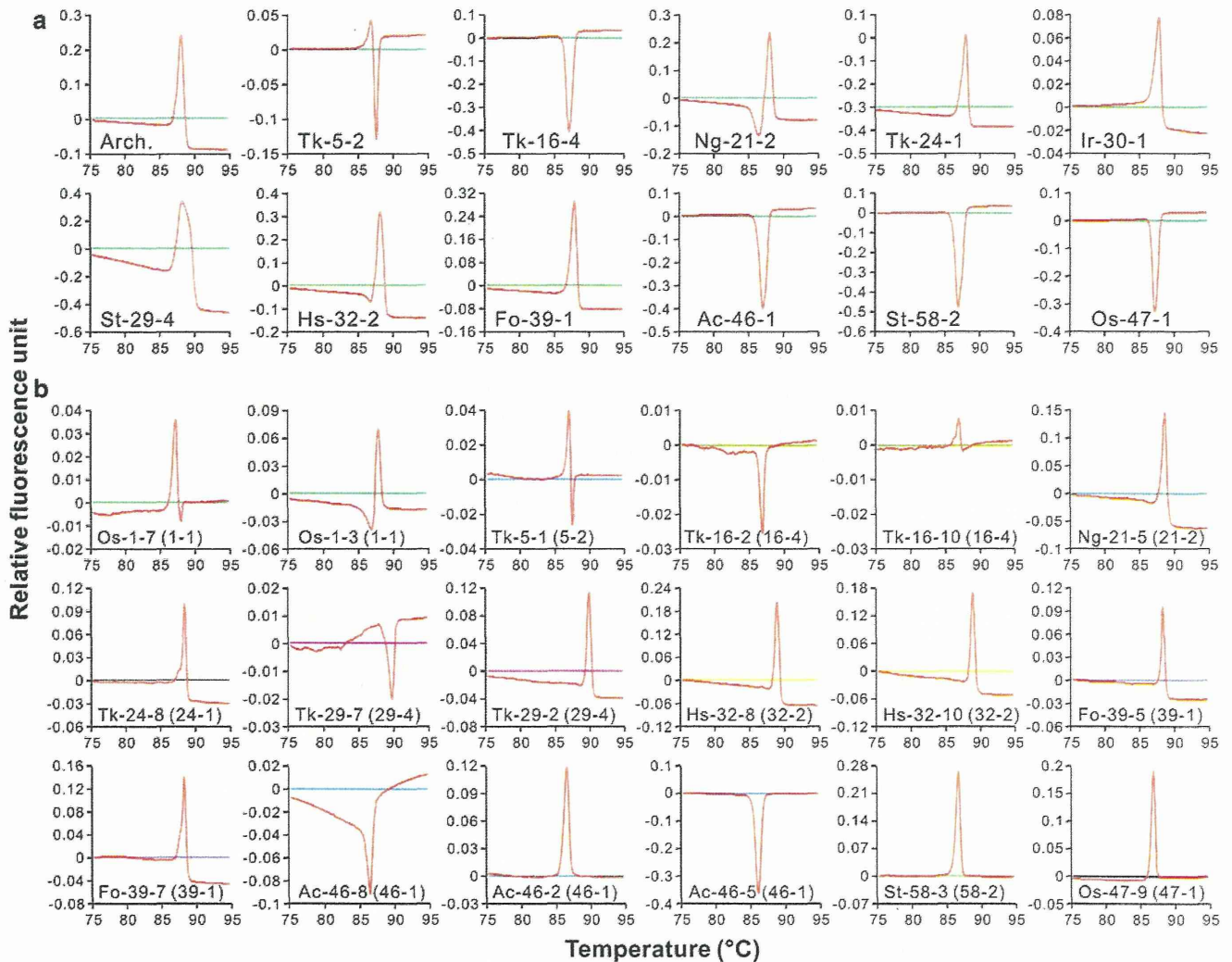


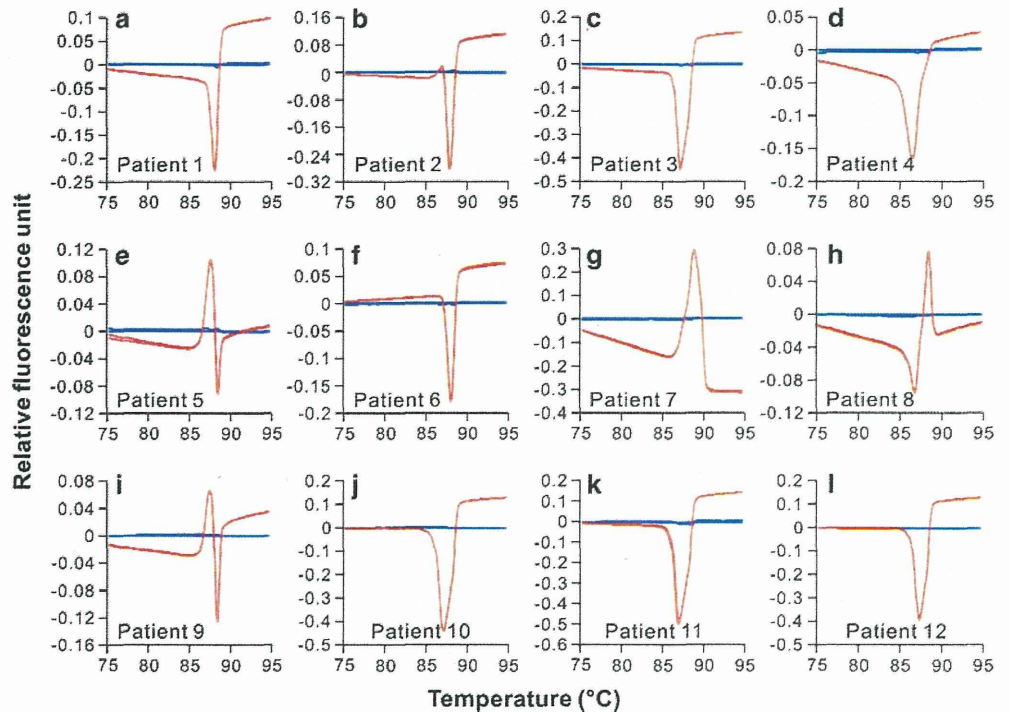
**Fig. 2** Comparisons of HRM profiles among the rearranged NCCRs cloned from different specimens or the same specimen from PML patients. The single-step PCR-HRM analyses were conducted using the archetype NCCR (Arch.) and the rearranged NCCR clones listed in Table 2 as described for Fig. 1. In panel a, the baseline data were obtained from NCCR clone Os-1-1 (green lines), and the HRM profiles of the representative NCCRs from different patients are

compared (red lines). In panel b, the HRM profiles of the rearranged NCCRs (red lines) were calculated with reference to those of the representative NCCRs cloned from the same patient (other colors). The scale on the y-axis differs from that in panel a. The baseline data are shown in parentheses (e.g., “1-1” indicates that the baseline data are obtained from clone Os-1-1 (color figure online))

In contrast, no amplification signals were obtained from any JCV-negative CSF specimens. It was also found that the HRM profiles of JCV variants in each specimen were similar to those of the cloned NCCRs (Fig. 1, red lines). The experiments shown in Fig. 4 were conducted to assess whether the nested PCR-HRM is able to distinguish the NCCR patterns of JCV DNA variants in clinical specimens. The nested-PCR HRM analyses were performed on CSF DNAs from PML patients after obtaining baseline data from each clinical sample as well as from the archetype JCV. The HRM profiles of the JCV variants from patients 2 to 4 (Fig. 4a, red lines) were different from those

from patient 1 (Fig. 4a, green line). The analyses shown in Fig. 4b were performed to determine whether the NCCR patterns could be numerically distinguished by the nested PCR-HRM assay in all combinations of CSF DNAs. The maximum values of the fluorescence differences from the baselines were determined as indicated in Fig. 4a. When the HRM data of CSF DNAs from each PML patient were used for the baseline, the HRM patterns of the NCCRs were different from each other. These data demonstrate that the nested PCR-HRM assay can distinguish the NCCR patterns of JCV variants in clinical specimens without the cloning and sequencing of viral DNA.

**Fig. 3** Comparisons of HRM patterns of NCCRs between the archetype JCV and JCV variants in CSF specimens from PML patients. The nested PCR-HRM assay targeting the NCCR was performed using the archetype JCV genome (blue lines) and JCV DNAs in CSFs from the patients listed in Table 1 (red lines) in duplicate. The differences in fluorescence were determined by comparison with the data of the archetype JCV. Similar results were obtained from two other experiments (color figure online)



## Discussion

In this study, two types of HRM assays were established in combination with single-step and nested PCRs for the NCCR scanning of cloned JCV DNA and JCV variants, respectively, in CSF specimens. The HRM analyses developed in this study are thought to be unique in that the virus variants can be discriminated by the patient-specific and hypervariable mutations in the NCCRs without nucleotide sequencing. Because of highly variable mutations, it is difficult to distinguish rearranged NCCRs using real-time PCR with a specific oligonucleotide probe. Recently, Ryschkewitsch *et al.* have reported a probe-based real-time PCR assay targeting a partial sequence within the archetype NCCR, which is frequently deleted in the rearranged NCCRs of PML-type JCV variants [35]. This probe-based PCR is highly sensitive and quantitative, and is similar to the PCR-HRM developed in this study in that both of these aim to distinguish the archetype JCV from the JCV variants with rearranged NCCRs. However, when we analyzed the primer and probe sequences used for the probe-based PCR *in silico*, it was noticed that several rearranged NCCRs of PML-type JCV contain target regions as shown in this study (clones Os-1-1, Os-1-7, Ng-21-2, Ng-21-5, and Ir-30-1) and in a previous report by Gosert *et al.* [19]. Thus, the possibility cannot be excluded that the probe-based PCR detects the rearranged NCCR as the archetype. If these NCCR patterns are dominant in the clinical specimens, the detected virus may be judged to be either the archetype or a mixture of the

archetype and PML-type viruses. In addition, the probe-based PCR assay cannot detect rearranged NCCRs, while the current PCR-HRM assays can differentiate the mutational patterns of the rearranged NCCRs.

An important aspect of the single-step PCR-HRM assay is that it is able to compare the NCCR patterns of cloned JCV DNA in about 1 hour. The differences in NCCR patterns can be measured rapidly and semi-automatically without sequencing and *in silico* analyses. The nucleotide sequencing analyses of NCCRs are generally performed using multiple clones from a single specimen, and the highly variable mutations have to be examined *in silico* by repeatedly aligning partial sequences to the archetype NCCR. Thus, the number of target clones can be reduced by using HRM scanning prior to sequence analysis. In addition, the present assay was able to distinguish the mutational patterns of multiple NCCRs cloned from CSF specimens from the same patient. The single-step PCR-HRM assay developed in the present study may serve as a quick and convenient tool for comparing the mutational patterns of JCV NCCRs, not only as part of PML diagnosis but also in various studies examining JCV variant populations. Although the amplification efficiency of the single-step PCR-HRM is low, the assay possesses one advantage in that the results are not influenced by contamination with small amounts of DNA when using high-copy plasmids as PCR templates.

Since the real-time PCR assay for JCV testing is generally designed to detect highly conserved regions within

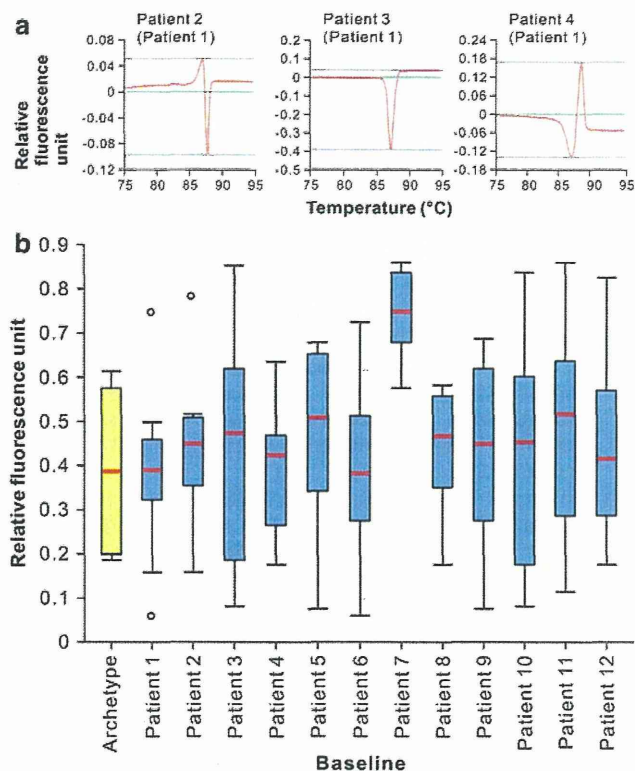


**Fig. 4** Differentiation of HRM profiles of JCV NCCRs among PML patients. The nested PCR-HRM analyses targeting NCCRs were performed as described in Fig. 3. In panel a, the HRM profiles of NCCR patterns in the CSF specimens from patients 2 to 4 (red lines) with reference to those from patient 1 (green lines) are shown to represent the maximum values of fluorescence differences (dotted lines). In panel b, the baseline data were collected from CSF DNA of one PML patient, as indicated below the x-axis (blue), and the fluorescence differences of other CSF samples are shown in box-and-whisker plots ( $n = 11$ ). The HRM profiles of all CSF samples with reference to the archetype JCV DNA are also shown (yellow,  $n = 12$ ). The red horizontal line within each box is the median; the lower and upper boundaries are the 25th and 75th percentiles, respectively; vertical whiskers extend over the range, and open circles show outliers (color figure online)

the viral genome [34, 36–38], sporadic contamination due to sample-to-sample carryover of positive control or JCV-positive specimens during sample processing, DNA extraction, and PCR template preparation is difficult to control by sequencing of the PCR product. As shown in Fig. 4, NCCR typing is thought to be useful to exclude the possibility of DNA contamination from JCV-positive specimens. For PCR amplification of the full-length NCCR, nested PCR was generally conducted due to the low amplification efficiency [14, 19, 28]. In agreement with previous reports, the authors could not find appropriate primers or cycle conditions for highly sensitive single-step PCR. Thus, the nested PCR-HRM analyses were performed to detect small amounts of PCR templates in clinical samples. Although this nested PCR-HRM assay requires

the pre-amplification of target sequences by conventional PCR, the NCCR patterns of CSF JCVs can be discriminated in a total of about 2 hours without cloning or sequencing. When NCCR typing is conducted routinely for diagnostic purposes, it is ideal that the procedures involving electrophoresis and plasmid cloning of the PCR products is minimized to eliminate the risk of DNA contamination. Since the HRM profiles of the CSF DNAs from PML patients were similar to those of the cloned NCCRs, the cloning and/or sequencing of target sequences can be omitted for NCCR typing by the use of the nested PCR-HRM. In addition, the absence of nonspecific amplification was confirmed in the current assay using more than 150 JCV-negative CSF samples. Since no specific treatment has yet been established for PML, restoration of the immune system is the only treatment option for the management of PML [1]. False-positive results in the routine PCR testing for JCV DNA may influence therapeutic interventions, especially in moderating immunosuppressive therapies in HIV-negative PML patients. This possibility can be reduced by the confirmation of PML using HRM analysis. Thus, HRM-based scanning serves as a powerful methodology, not only for basic research but also for PML diagnosis, when combined with routine real-time PCR testing.

**Acknowledgments** The authors are grateful to all study participants and physicians who contributed to the present study. This work was partly supported by Grants-in-Aid for the Research on HIV/AIDS (H24-AIDS-Wakate-002), the Research for Intractable Infectious Diseases in Organ Transplant Recipients (H21-Shinko-Ippan-009), and the Research Committee of Prion Disease and Slow Virus Infection (H22-Nanchi-Ippan-013) from the Ministry of Health, Labour and Welfare of Japan.

**Conflict of interest** The authors declare that they have no conflict of interest.

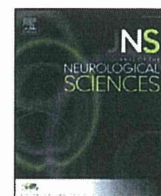
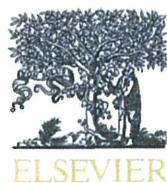
## References

1. Brew BJ, Davies NW, Cinque P, Clifford DB, Nath A (2010) Progressive multifocal leukoencephalopathy and other forms of JC virus disease. *Nat Rev Neurol* 6:667–679. doi:10.1038/nrneurol.2010.164
2. Tan CS, Korolnik IJ (2010) Progressive multifocal leukoencephalopathy and other disorders caused by JC virus: clinical features and pathogenesis. *Lancet Neurol* 9:425–437. doi:10.1016/s1474-4422(10)70040-5
3. Shishido-Hara Y (2010) Progressive multifocal leukoencephalopathy and promyelocytic leukemia nuclear bodies: a review of clinical, neuropathological, and virological aspects of JC virus-induced demyelinating disease. *Acta Neuropathol* 120:403–417. doi:10.1007/s00401-010-0694-x
4. Knowles WA, Pipkin P, Andrews N, Vyse A, Minor P, Brown DW, Miller E (2003) Population-based study of antibody to the human polyomaviruses BKV and JCV and the simian polyomavirus SV40. *J Med Virol* 71:115–123. doi:10.1002/jmv.10450

5. Major EO (2010) Progressive multifocal leukoencephalopathy in patients on immunomodulatory therapies. *Annu Rev Med* 61:35–47. doi:[10.1146/annurev.med.080708.082655](https://doi.org/10.1146/annurev.med.080708.082655)
6. Chen Y, Bord E, Tompkins T, Müller J, Tan CS, Kinkel RP, Stein MC, Viscidi RP, Ngo LH, Koralnik IJ (2009) Asymptomatic reactivation of JC virus in patients treated with natalizumab. *N Engl J Med* 361:1067–1074. doi:[10.1056/nejmoa0904267](https://doi.org/10.1056/nejmoa0904267)
7. Cinque P, Koralnik IJ, Gerevini S, Miro JM, Price RW (2009) Progressive multifocal leukoencephalopathy in HIV-1 infection. *Lancet Infect Dis* 9:625–636. doi:[10.1016/s1473-3099\(09\)70226-9](https://doi.org/10.1016/s1473-3099(09)70226-9)
8. Marzocchetti A, Di Giambenedetto S, Cingolani A, Ammassari A, Cauda R, De Luca A (2005) Reduced rate of diagnostic positive detection of JC virus DNA in cerebrospinal fluid in cases of suspected progressive multifocal leukoencephalopathy in the era of potent antiretroviral therapy. *J Clin Microbiol* 43:4175–4177. doi:[10.1128/jcm.43.8.4175-4177](https://doi.org/10.1128/jcm.43.8.4175-4177)
9. Espy MJ, Uhl JR, Sloan LM, Buckwalter SP, Jones MF, Vetter EA, Yao JD, Wengenack NL, Rosenblatt JE, Cockerill FR 3rd, Smith TF (2006) Real-time PCR in clinical microbiology: applications for routine laboratory testing. *Clin Microbiol Rev* 19:165–256. doi:[10.1128/cmr.19.1.165-256](https://doi.org/10.1128/cmr.19.1.165-256)
10. Jensen PN, Major EO (2001) A classification scheme for human polyomavirus JCV variants based on the nucleotide sequence of the noncoding regulatory region. *J Neurovirol* 7:280–287. doi:[10.1080/13550280152537102](https://doi.org/10.1080/13550280152537102)
11. Marshall LJ, Dunham L, Major EO (2010) Transcription factor Spi-B binds unique sequences present in the tandem repeat promoter/enhancer of JC virus and supports viral activity. *J Gen Virol* 91:3042–3052. doi:[10.1099/vir.0.023184-0](https://doi.org/10.1099/vir.0.023184-0)
12. Imperiale MJ, Major EO (2007) Polyomaviruses. In: Knipe DM, Howley PM, Griffin DE, Lamb RA, Martin MA, Roizman B, Straus SE (eds) *Fields virology*, 5th edn. Lippincott Williams & Wilkins, Philadelphia, pp 2263–2298
13. Yogo Y, Kitamura T, Sugimoto C, Ueki T, Aso Y, Hara K, Taguchi F (1990) Isolation of a possible archetypal JC virus DNA sequence from nonimmunocompromised individuals. *J Virol* 64:3139–3143
14. Tan CS, Ellis LC, Wuthrich C, Ngo L, Broge TA Jr, Saint-Aubyn J, Miller JS, Koralnik IJ (2010) JC virus latency in the brain and extraneural organs of patients with and without progressive multifocal leukoencephalopathy. *J Virol* 84:9200–9209. doi:[10.1128/jvi.00609-10](https://doi.org/10.1128/jvi.00609-10)
15. Seth P, Diaz F, Major EO (2003) Advances in the biology of JC virus and induction of progressive multifocal leukoencephalopathy. *J Neurovirol* 9:236–246. doi:[10.1080/13550280390194019](https://doi.org/10.1080/13550280390194019)
16. Ault GS, Stoner GL (1993) Human polyomavirus JC promoter/enhancer rearrangement patterns from progressive multifocal leukoencephalopathy brain are unique derivatives of a single archetypal structure. *J Gen Virol* 74:1499–1507. doi:[10.1099/0022-1317-74-8-1499](https://doi.org/10.1099/0022-1317-74-8-1499)
17. Yogo Y, Sugimoto C (2001) The archetype concept and regulatory region rearrangement. In: Khalili K, Stoner GL (eds) *Human polyomaviruses: molecular and clinical perspectives*. Wiley-Liss, New York, pp 127–148
18. Marshall LJ, Major EO (2010) Molecular regulation of JC virus tropism: insights into potential therapeutic targets for progressive multifocal leukoencephalopathy. *J Neuroimmune Pharmacol* 5:404–417. doi:[10.1007/s11481-010-9203-1](https://doi.org/10.1007/s11481-010-9203-1)
19. Gosert R, Kardas P, Major EO, Hirsch HH (2010) Rearranged JC virus noncoding control regions found in progressive multifocal leukoencephalopathy patient samples increase virus early gene expression and replication rate. *J Virol* 84:10448–10456. doi:[10.1128/jvi.00614-10](https://doi.org/10.1128/jvi.00614-10)
20. Agostini HT, Ryschkewitsch CF, Singer EJ, Stoner GL (1997) JC virus regulatory region rearrangements and genotypes in progressive multifocal leukoencephalopathy: two independent aspects of virus variation. *J Gen Virol* 78:659–664
21. Reid CE, Li H, Sur G, Carmillo P, Bushnell S, Tizard R, McAuliffe M, Tonkin C, Simon K, Goelz S, Cinque P, Gorelik L, Carulli JP (2011) Sequencing and analysis of JC virus DNA from natalizumab-treated PML patients. *J Infect Dis* 204:237–244. doi:[10.1093/infdis/jir256](https://doi.org/10.1093/infdis/jir256)
22. Roux D, Bouldouyre MA, Mercier-Delarue S, Seilhean D, Zagdanski AM, Delaugerre C, Simon F, Molina JM, Legoff J (2011) JC virus variant associated with cerebellar atrophy in a patient with AIDS. *J Clin Microbiol* 49:2196–2199. doi:[10.1128/jcm.02057-10](https://doi.org/10.1128/jcm.02057-10)
23. Delbue S, Elia F, Carloni C, Tavazzi E, Marchioni E, Carluccio S, Signorini L, Novati S, Maserati R, Ferrante P (2012) JC virus load in cerebrospinal fluid and transcriptional control region rearrangements may predict the clinical course of progressive multifocal leukoencephalopathy. *J Cell Physiol* 227:3511–3517. doi:[10.1002/jcp.24051](https://doi.org/10.1002/jcp.24051)
24. Nakamichi K, Kishida S, Tanaka K, Suganuma A, Sano Y, Sano H, Kanda T, Maeda N, Kira J, Itoh A, Kato N, Tomimoto H, Kurane I, Lim CK, Mizusawa H, Saijo M (2013) Sequential changes in the non-coding control region sequences of JC polyomaviruses from the cerebrospinal fluid of patients with progressive multifocal leukoencephalopathy. *Arch Virol* 158:639–650. doi:[10.1007/s00705-012-1532-3](https://doi.org/10.1007/s00705-012-1532-3)
25. Ciappi S, Azzi A, De Santis R, Leoncini F, Sterrantino G, Mazzotta F, Mecocci L (1999) Archetypal and rearranged sequences of human polyomavirus JC transcription control region in peripheral blood leukocytes and in cerebrospinal fluid. *J Gen Virol* 80:1017–1023
26. Iida T, Kitamura T, Guo J, Taguchi F, Aso Y, Nagashima K, Yogo Y (1993) Origin of JC polyomavirus variants associated with progressive multifocal leukoencephalopathy. *Proc Natl Acad Sci USA* 90:5062–5065. doi:[10.1073/pnas.90.11.5062](https://doi.org/10.1073/pnas.90.11.5062)
27. Marzocchetti A, Wuthrich C, Tan CS, Tompkins T, Bernal-Cano F, Bhargava P, Ropper AH, Koralnik IJ (2008) Rearrangement of the JC virus regulatory region sequence in the bone marrow of a patient with rheumatoid arthritis and progressive multifocal leukoencephalopathy. *J Neurovirol* 14:455–458. doi:[10.1080/13550280802356837](https://doi.org/10.1080/13550280802356837)
28. Sugimoto C, Ito D, Tanaka K, Matsuda H, Saito H, Sakai H, Fujihara K, Itoyama Y, Yamada T, Kira J, Matsumoto R, Mori M, Nagashima K, Yogo Y (1998) Amplification of JC virus regulatory DNA sequences from cerebrospinal fluid: diagnostic value for progressive multifocal leukoencephalopathy. *Arch Virol* 143:249–262. doi:[10.1007/s007050050284](https://doi.org/10.1007/s007050050284)
29. Yasuda Y, Yabe H, Inoue H, Shimizu T, Yabe M, Yogo Y, Kato S (2003) Comparison of PCR-amplified JC virus control region sequences from multiple brain regions in PML. *Neurology* 61:1617–1619. doi:[10.1212/01.wnl.0000096147.47128.7d](https://doi.org/10.1212/01.wnl.0000096147.47128.7d)
30. Reed GH, Kent JO, Wittwer CT (2007) High-resolution DNA melting analysis for simple and efficient molecular diagnostics. *Pharmacogenomics* 8:597–608. doi:[10.2217/14622416.8.6.597](https://doi.org/10.2217/14622416.8.6.597)
31. Tong SY, Giffard PM (2012) Microbiological applications of high-resolution melting analysis. *J Clin Microbiol* 50:3418–3421. doi:[10.1128/jcm.01709-12](https://doi.org/10.1128/jcm.01709-12)
32. Nakamichi K, Mizusawa H, Yamada M, Kishida S, Miura Y, Shimokawa T, Takasaki T, Lim CK, Kurane I, Saijo M (2012) Characteristics of progressive multifocal leukoencephalopathy clarified through internet-assisted laboratory surveillance in Japan. *BMC Neurol* 12:121. doi:[10.1186/1471-2377-12-121](https://doi.org/10.1186/1471-2377-12-121)
33. Yogo Y, Guo J, Iida T, Satoh K, Taguchi F, Takahashi H, Hall WW, Nagashima K (1994) Occurrence of multiple JC virus variants with distinctive regulatory sequences in the brain of a single patient with progressive multifocal leukoencephalopathy. *Virus Genes* 8:99–105. doi:[10.1007/bf01703608](https://doi.org/10.1007/bf01703608)



34. Nakamichi K, Kurane I, Saijo M (2011) Evaluation of a quantitative real-time PCR assay for the detection of JC polyomavirus DNA in cerebrospinal fluid without nucleic acid extraction. *Jpn J Infect Dis* 64:211–216
35. Ryschkewitsch CF, Jensen PN, Major EO (2013) Multiplex qPCR assay for ultra sensitive detection of JCV DNA with simultaneous identification of genotypes that discriminates non-virulent from virulent variants. *J Clin Virol* 57:243–248. doi:[10.1016/j.jcv.2013.03.009](https://doi.org/10.1016/j.jcv.2013.03.009)
36. Ryschkewitsch C, Jensen P, Hou J, Fahle G, Fischer S, Major EO (2004) Comparison of PCR-southern hybridization and quantitative real-time PCR for the detection of JC and BK viral nucleotide sequences in urine and cerebrospinal fluid. *J Virol Methods* 121:217–221. doi:[10.1016/j.jviromet.2004.06.021](https://doi.org/10.1016/j.jviromet.2004.06.021)
37. Sehmani L, Kabamba-Mukadi B, Vandenbroucke AT, Bodeus M, Goubau P (2006) Specific and quantitative detection of human polyomaviruses BKV and JCV by LightCycler real-time PCR. *J Clin Virol* 36:159–162. doi:[10.1016/j.jcv.2006.01.013](https://doi.org/10.1016/j.jcv.2006.01.013)
38. Dumonceaux TJ, Mesa C, Severini A (2008) Internally controlled triplex quantitative PCR assay for human polyomaviruses JC and BK. *J Clin Microbiol* 46:2829–2836. doi:[10.1128/jcm.00844-08](https://doi.org/10.1128/jcm.00844-08)



## Short communication

## Favorable outcome after withdrawal of immunosuppressant therapy in progressive multifocal leukoencephalopathy after renal transplantation: Case report and literature review



Hiroya Ohara <sup>a</sup>, Hiroshi Kataoka <sup>a,\*</sup>, Kazuo Nakamichi <sup>b</sup>, Masayuki Saijo <sup>b</sup>, Satoshi Ueno <sup>a</sup>

<sup>a</sup> Department of Neurology, Nara Medical University, Kashihara, Nara, Japan

<sup>b</sup> Department of Virology 1, National Institute of Infectious Diseases, Shinjuku-ku, Tokyo, Japan

## ARTICLE INFO

## Article history:

Received 5 November 2013

Received in revised form 20 February 2014

Accepted 25 March 2014

Available online 2 April 2014

## Keywords:

PML

Renal transplantation

JC virus

Immunosuppressant

Therapy

## ABSTRACT

Progressive multifocal leukoencephalopathy (PML) is a fatal demyelinating disease caused by the JC polyomavirus (JCV). Most patients with PML after renal transplantation have had poor outcomes. We describe a patient with PML after renal transplantation who had a good response to the withdrawal of immunosuppressant therapy. We performed quantitative real-time PCR testing for JCV DNA in cerebrospinal fluid (CSF), and assessed mutation of the JCV genome detected in the CSF. At the same time, we checked cranial magnetic resonance imaging (MRI). Immunosuppressant therapy was discontinued immediately. The MRI scan that followed showed markedly decreased numbers of high intensity signals, and the results of real-time PCR for JCV DNA in CSF became negative. The patient had no other neurological deficits. Withdrawal of immunosuppressant treatment has a beneficial effect on the course of PML after renal transplantation, and quantitative PCR may facilitate the immediate withdrawal of immunosuppressant agents.

© 2014 Elsevier B.V. All rights reserved.

### 1. Introduction

Progressive multifocal leukoencephalopathy (PML) is a fatal demyelinating disease caused by the JC polyomavirus (JCV) [13], and survivors often have severe neurological sequelae. PML has been closely associated with profound immunodeficiency in the setting of human immunodeficiency virus (HIV) infection, hematologic malignancies, or autoimmune disorders. Rarely, PML has been reported in solid-organ transplant recipients. The estimated incidence in recipients of renal transplants is 0.027% [10]. Most patients with PML after renal transplantation have had poor outcomes [7]. We describe a patient with PML after renal transplantation who had a good response to the withdrawal of immunosuppressant therapy.

### 2. Case report

A 51-year-old woman had undergone living-donor renal transplantation at the age of 22 years because of chronic renal failure with glomerular nephritis. At 27 years of age, hemodialysis was resumed

because of chronic allograft nephropathy. At 45 years of age, renal transplantation was performed again. The titer of panel reactive antibody (PRA) class I against human leukocyte antigen of the donor was as high as a rate of 60.1%. The patient received intravenous immunoglobulin (500 mg/kg/day, 5 days) and plasmapheresis (5 days) with oral basiliximab (40 mg twice) to prevent antibody-mediated rejection. Neutrophilic infiltration of glomeruli and peritubular capillaries was confirmed histologically. Subsequently, cyclosporine (100 mg/day), mycophenolate mofetil (MMF, 1000 mg/day), and prednisone (10 mg/day) were given for 5 years.

In February 2012, she noticed numbness on the left side of the face and the left limbs and was admitted to our hospital. Neck stiffness was absent, and she was fully oriented. Except for mild weakness and involuntary movements in the left forearm, other neurological findings were normal. The results of routine serum laboratory tests were normal, including renal function, and HIV was negative. Initial cranial magnetic resonance imaging (MRI) on day 2 after admission showed abnormally high signal intensity in the right frontal and temporal lobes (Fig. 1a and b). The white cell count and the protein concentration in cerebrospinal fluid (CSF) were 5 cells/mm<sup>3</sup> and 44 mg/dl, respectively. Quantitative real-time PCR testing for JCV DNA in CSF was positive, and the JCV DNA load was 12,623 copies/ml. On nucleotide sequence analysis, apparent mutations (deletions, insertions, or both) characteristic of PML-type virus [9] were found in the non-coding control region of the JCV genome in CSF (Fig. 2). PML was therefore diagnosed. The weakness

\* Corresponding author at: Department of Neurology, Nara Medical University, 840 Shijo-cho, Kashihara, Nara 634-8522, Japan. Tel.: +81 744 29 8860; fax: +81 744 24-6065.

E-mail address: [hk55@naramed-u.ac.jp](mailto:hk55@naramed-u.ac.jp) (H. Kataoka).